Author Manuscript

Author Manuscript

Author Manuscript

Author Manuscript

HHS Public Access

Author manuscript

Science. Author manuscript; available in PMC 2017 July 26.

Published in final edited form as:

Science. 2017 April 14; 356(6334): 194–197. doi:10.1126/science.aal3059.

Architecture of a transcribing-translating expressome

R. Kohler[1], **R.A. Mooney**[2], **D.J. Mills**[3], **R. Landick**[2,*], and **P. Cramer**[1,*]

[1]Max Planck Institute for Biophysical Chemistry, Department of Molecular Biology, Am Fassberg 11, 37077 Göttingen, Germany

[2]Department of Biochemistry, University of Wisconsin-Madison, Madison, WI 53706, USA

[3]Max Planck Institute for Biophysics, Department of Structural Biology, Max-von-Laue-Str. 3, 60438 Frankfurt am Main, Germany

Abstract

DNA transcription is functionally coupled to mRNA translation in bacteria, but how this is achieved remains unclear. Here we show that RNA polymerase (RNAP) and the ribosome of E. coli can form a defined transcribing and translating 'expressome' complex. The cryo-electron microscopic structure of the expressome reveals continuous protection of ~30 nucleotides of mRNA extending from the RNAP active center to the ribosome decoding center. The RNAP-ribosome interface includes the RNAP subunit α C-terminal domain, which is required for RNAP-ribosome interaction in vitro and for pronounced cell growth defects upon translation inhibition in vivo, consistent with its function in transcription-translation coupling. The expressome structure can only form during transcription elongation and explains how translation can prevent transcriptional pausing, backtracking, and termination.

Main Text

Gene expression in all organisms involves transcription and translation. During transcription, RNA polymerase (RNAP) transcribes DNA into messenger RNA (mRNA). During translation, the ribosome uses mRNA as a template for protein synthesis. Half a century ago, it was predicted that transcription and translation are linked in prokaryotic cells (1). Early electron microscopy showed transcribing RNAP in close proximity to ribosomes in *E. coli* (2). When RNAP produces mRNA containing a ribosome-binding sequence (RBS), translation can initiate and prevent transcription termination (3). Translation inhibition leads to increased RNAP pausing, showing that transcription and translation are kinetically coupled (4, 5). Thus a pioneering ribosome on the nascent mRNA promotes transcription and governs the overall rate of gene expression. It was suggested that NusG or related

*Correspondence: landick@bact.wisc.edu; patrick.cramer@mpibpc.mpg.de.

Author contributions: R.K. designed experiments and performed interaction assays, electron microscopy and data analysis. R.A.M. and R.L. prepared *E. coli* RNAP and performed *in vivo* and genome-wide experiments. D.J.M. supervised EM data collection. P.C. and R.L. designed and supervised research. R.K. and P.C. prepared the manuscript with input from all authors.

One Sentence Summary:
The structure of a RNA polymerase-ribosome complex suggests the molecular basis for transcription-translation coupling.

Author Manuscript Author Manuscript Author Manuscript Author Manuscript

proteins form a physical bridge between RNAP and the ribosome (6), but the structural basis for transcription-translation coupling is unknown.

We assumed that transcription-translation coupling requires formation of a structurally defined, functional RNAP-ribosome complex that we call here ‘expressome’. To investigate whether the expressome exists, we formed a stalled transcription elongation complex (EC) from *E. coli* RNAP and a DNA-RNA scaffold with a RBS in the RNA 5′-region, and used this EC as a substrate for translation (Methods, Supplementary Materials). The ribosome translated the RNA until it encountered the stalled RNAP (Fig. 1). The resulting complex was purified by affinity purification and gradient centrifugation.

EM imaging of purified complexes after negative staining revealed ribosomes with an additional density on the small (30S) ribosomal subunit that corresponded in size to RNAP (Fig. S1). Cryo-EM images collected with a direct electron detector led to 2D particle class averages and an unclassified 3D reconstruction that confirmed the additional density on ribosomes (Fig. S1B–D). Unsupervised local 3D classification of 104,763 ribosome particles yielded a class of 15,085 particles with the RNAP EC in a well-defined orientation, indicating that the *in vitro* preparation led to the formation of an expressome (Fig. S2). We obtained a cryo-EM reconstruction of the *E. coli* expressome at a resolution of 7.6 Å (FSC=0.143, Fig. S3A).

The cryo-EM reconstruction (Fig. S3) enabled building of a backbone model of the expressome (Fig. 2). Crystal structures for ribosomal subunits (7) were fitted into the electron density. The ribosome shows only local structural changes and occupies a post-translocation state resembling state ‘post 2’ (8). The P-site tRNA has good density (Fig. S4A) and shows mRNA codon-anticodon interactions. The E-site tRNA shows weaker density, likely because it is partially lost during purification (9). Density for the nascent protein is visible in the polypeptide tunnel (Fig. S4A), showing that the ribosome was translating before cryo-EM analysis. The crystal structure of *E. coli* RNAP (10) was fitted automatically and unambiguously (cross-correlation = 0.87) to the density on the 30S subunit. Downstream DNA and the DNA-RNA hybrid within RNAP were placed into densities at known locations (11).

In the derived architectural model of the expressome, the RNA exit region of RNAP docks onto the site of entry to the ribosomal mRNA-binding channel between ribosomal proteins S3, S4 and S5 (Fig. 2B, 3A). Nascent mRNA exiting from RNAP enters straight into the ribosome, consistent with seamless mRNA protection in the expressome. The mRNA was traced through continuous electron density, which was less defined only for nucleotides at registers ~12–18 at the interface between RNAP and the ribosome (Fig 2C). Around 30 nucleotides of RNA suffice to span the sites of RNA synthesis and decoding, consistent with prior results (12). The mRNA is defined in the decoding center and until register ~32 before it exits the narrow RNA tunnel in the region between ribosomal proteins S2, S7, S18 and S21.

The RNAP uses surfaces on four of its five subunits to contact the 30S subunit (Fig. 3). The interface is formed by conserved elements of RNAP (13) and the ribosome (14). The N-

Author Manuscript Author Manuscript Author Manuscript Author Manuscript

terminal domain (NTD) of RNAP subunit α1 interacts with ribosomal proteins S3 and S10; the RNAP flap domain contacts S3, S4, and the 16S ribosomal RNA at helix 18; the RNAP β SI2 motif (5byh, chain C, residues ~ 944–1040, aka βi9, Fig. 3B) contacts RNA helix 33 and ribosomal protein S3; the RNAP subunit β′ clamp domain contacts proteins S4 and S5; and the RNAP subunit ω contacts protein S2.

The RNAP-ribosome interface contained an additional electron density (Fig. 3B) that we hypothesize belongs to the RNAP α subunit C-terminal domains (αCTDs), because all other domains were assigned. This density could accommodate αCTDs from both adjacent α subunits. Although its quality was not sufficient for modeling, we note that this density would position the αCTDs near 16S rRNA helix 39. To investigate if the αCTDs are involved in RNAP-ribosome interaction, we tested whether isolated *E. coli* RNAP and ribosome particles interact *in vitro*. We observed formation of an RNAP-ribosome complex that was stable during sucrose-gradient centrifugation (Fig. 4A, lane 1; Fig. S5). We repeated the interaction assay with an RNAP variant that lacked both αCTDs (RNAPΔαCTD), and ribosome-RNAP binding was essentially abolished (Fig 4A, lane 3). In contrast, deletion of the RNAP region SI2 (RNAPΔSI2), which forms a minor contact with the ribosome, did not reduce binding (Fig 4A, lane 2). Thus the αCTD, but not SI2, is required for RNAP-ribosome interaction.

To investigate the effect of the αCTD-ribosome interaction *in vivo*, we expressed wild-type and ΔαCTD RNAPs from an arabinose-inducible plasmid in early exponential phase cells growing in minimal medium (Fig. 4B). After arabinose induction for 40 min, ~80% of cellular RNAP lacked the αCTD, but cell growth remained nearly normal (Fig. S6). To compromise translation, we added chloramphenicol (Cm) at 0.5–20 μg/ml. The growth rate of cells containing ΔαCTD RNAP was inhibited to a lesser extent by Cm than cells containing wild-type RNAP (Fig. 4C, Fig. S6), suggesting that disruption of the RNAP-ribosome interaction by removal of αCTD reduced the effect of translation inhibition on cell growth. At higher Cm concentrations, cell density decreased, indicating cell death occurring to a greater extent in wild-type cells. Greater cell viability in ΔαCTD RNAP cells was not due to loss of Rho inhibition. At shorter times inhibiting Rho with bicyclomycin (Bcm) did not aid wild-type cells and increased the difference between wild-type and ΔαCTD cells. At longer times, Rho inhibition was synergistic with Cm in lowering cell density. Consistent with these findings, transcription of *lacZ* by ΔαCTD RNAP progressed further in the presence of Cm than did transcription by wild-type RNAP, as assayed by chromatin immunoprecipitation after addition of ITPG and Cm (Fig. S7).

Although indirect, these *in vivo* results are consistent with an αCTD-mediated ribosome-RNAP interaction slowing transcription and increasing transcriptional arrest upon Cm addition. We suggest that an increase in RNAP arrest caused by interaction with inhibited ribosomes may increase replisome-RNAP collisions and thus interfere with DNA replication (15), causing cell lethality.

The αCTDs are flexibly connected to RNAP (16) and bind to promoters and regulatory proteins during transcription initiation (17–20), suggesting that the expressome can only form after the transition from transcription initiation to elongation. Indeed, modeling shows

Author Manuscript Author Manuscript Author Manuscript Author Manuscript

that the RNAP initiation factors sigma70 (21), sigma54 (10) and sigma38 (22) cannot bind to RNAP in the expressome (Fig. S4B). In contrast, binding of the RNAP elongation factors GreA, GreB, NusG, and RfaH to RNAP is possible after expressome formation (23–25) (Fig. S4C). However, RNAP-bound NusG or RfaH cannot simultaneously bind the 30S protein S10 in the expressome (6, 26), because the NusG/RfaH linker is too short (Fig. 3B, Fig. S4C).

The expressome structure also explains how a translating ribosome in the wake of RNAP prevents transcriptional pausing, backtracking, and termination (4). Pausing and backtracking require RNAP to stall and reverse thread the RNA, which is prevented by a translating ribosome that binds RNAP and pulls on the exiting nascent RNA. Modeling shows that binding of the transcription termination factor NusA (27) to RNAP is not possible in the expressome due to a predicted clash with the 30S subunit; nor is NusA able to prevent ribosome-RNAP binding through its contacts to the αCTD (Fig. S5A). Similarly, the transcription termination factor Rho cannot approach RNAP because it binds to exiting RNA that is shielded by the ribosome. The RNAP-ribosome interface also does not leave space for the formation of a terminator RNA hairpin, consistent with the ability of ribosomes to block intrinsic termination (28).

Whereas these results indicate that the expressome can only form during transcription elongation, further modeling suggests that translation cycles can occur within the expressome (Fig. S4B, C). The surface of the ribosome that interacts with RNAP in the expressome is not used by known ribosome-binding factors. Factors for translation initiation, elongation, termination, and for ribosome release and recycling, all bind near the ribosome subunit interface. RNAP binding at the observed surface is however predicted to be mutually exclusive with ribosome dimerization that occurs for ribosome storage (29) and possibly interferes with binding of transfer-messenger RNA that functions in ribosome recycling (30).

The structurally defined, functional expressome complex visualizes the central dogma of molecular biology within a single framework, and suggests a basis of transcription-translation coupling. The conservation of structural elements at the RNAP-ribosome interface may indicate that expressomes can form in all prokaryotes. Superposition of archaeal RNAP and ribosome onto our structure (Fig. S4D) leads only to minor clashes, suggesting that archaea may contain expressomes. In contrast, superposition with eukaryotic RNAP II and ribosome leads to steric clashes (Fig. S4E), consistent with rapid evolution of RNAP and ribosome surfaces after the separation of transcription and translation in two cellular compartments.

Supplementary Material

Refer to Web version on PubMed Central for supplementary material.

Acknowledgments

We thank Werner Kühlbrandt for access to a Titan electron microscope. We thank D. Haselbach, H. Stark and S. Prinz for help with grid preparation and negative stain data collection. We thank D. Kostrewa and C. Berecky for

Author Manuscript Author Manuscript Author Manuscript Author Manuscript

help. R. K. was supported by the European Commission (FP7-PEOPLE-IEF). P.C. was supported by the Deutsche Forschungsgemeinschaft (SFB860), the advanced grants 'TRANSIT' and 'TRANSREGULON' of the European Research Council, and the Volkswagen Foundation. An electron density map of the expressome with fitted structures, and the map for the ribosome with improved S1 density were deposited in the EM data base (accession codes EMD-3580 and EMD-3579, respectively).

References and Notes

1. Byrne R, Levin JG, Bladen HA, Nirenberg MW. The in Vitro Formation of a DNA-Ribosome Complex. Proceedings of the National Academy of Sciences of the United States of America. 1964; 52:140–148. [PubMed: 14192650]
2. Miller OL Jr, Hamkalo BA, Thomas CA Jr. Visualization of bacterial genes in action. Science. 1970; 169:392–395. [PubMed: 4915822]
3. Adhya S, Gottesman M. Control of transcription termination. Annual review of biochemistry. 47
4. Proshkin S, Rahmouni AR, Mironov A, Nudler E. Cooperation between translating ribosomes and RNA polymerase in transcription elongation. Science. 2010; 328:504–508. [PubMed: 20413502]
5. Landick R, Carey J, Yanofsky C. Translation activates the paused transcription complex and restores transcription of the trp operon leader region. Proceedings of the National Academy of Sciences of the United States of America. 1985; 82:4663–4667. [PubMed: 2991886]
6. Burmann BM, Schweimer K, Luo X, Wahl MC, Stitt BL, Gottesman ME, Rosch P. A NusE:NusG complex links transcription and translation. Science. 2010; 328:501–504. [PubMed: 20413501]
7. Schuwirth BS, Borovinskaya MA, Hau CW, Zhang W, Vila-Sanjurjo A, Holton JM, Cate JH. Structures of the bacterial ribosome at 3.5 A resolution. Science. 2005; 310:827–834. [PubMed: 16272117]
8. Fischer N, Konevega AL, Wintermeyer W, Rodnina MV, Stark H. Ribosome dynamics and tRNA movement by time-resolved electron cryomicroscopy. Nature. 2010; 466:329–333. [PubMed: 20631791]
9. Deeng J, Chan KY, van der Sluis EO, Berninghausen O, Han W, Gumbart J, Schulten K, Beatrix B, Beckmann R. Dynamic Behavior of Trigger Factor on the Ribosome. Journal of molecular biology. 2016; 428:3588–3602. [PubMed: 27320387]
10. Yang Y, Darbari VC, Zhang N, Lu D, Glyde R, Wang YP, Winkelman JT, Gourse RL, Murakami KS, Buck M, Zhang X. TRANSCRIPTION. Structures of the RNA polymerase-sigma54 reveal new and conserved regulatory strategies. Science. 2015; 349:882–885. [PubMed: 26293966]
11. Vassylyev DG, Vassylyeva MN, Zhang J, Palangat M, Artsimovitch I, Landick R. Structural basis for substrate loading in bacterial RNA polymerase. Nature. 2007; 448:163–168. [PubMed: 17581591]
12. Castro-Roa D, Zenkin N. In vitro experimental system for analysis of transcription-translation coupling. Nucleic acids research. 2012; 40(e45) published online EpubMar (10.1093/nar/gkr1262).
13. Murakami KS, Darst SA. Bacterial RNA polymerases: the wholo story. Current opinion in structural biology. 2003; 13:31–39. [PubMed: 12581657]
14. Ban N, Beckmann R, Cate JH, Dinman JD, Dragon F, Ellis SR, Lafontaine DL, Lindahl L, Liljas A, Lipton JM, McAlear MA, Moore PB, Noller HF, Ortega J, Panse VG, Ramakrishnan V, Spahn CM, Steitz TA, Tchorzewski M, Tollervey D, Warren AJ, Williamson JR, Wilson D, Yonath A, Yusupov M. A new system for naming ribosomal proteins. Current opinion in structural biology. 2014; 24:165–169. [PubMed: 24524803]
15. Zhang Y, Mooney RA, Grass JA, Sivaramakrishnan P, Herman C, Landick R, Wang JD. DksA guards elongating RNA polymerase against ribosome-stalling-induced arrest. Molecular cell. 2014; 53:766–778. [PubMed: 24606919]
16. Zhang G, Campbell EA, Minakhin L, Richter C, Severinov K, Darst SA. Crystal structure of Thermus aquaticus core RNA polymerase at 3.3 A resolution. Cell. 1999; 98:811–824. [PubMed: 10499798]
17. Benoff B, Yang H, Lawson CL, Parkinson G, Liu J, Blatter E, Ebright YW, Berman HM, Ebright RH. Structural basis of transcription activation: the CAP-alpha CTD-DNA complex. Science. 2002; 297:1562–1566. [PubMed: 12202833]

Author Manuscript Author Manuscript Author Manuscript Author Manuscript

18. Dangi B, Gronenborn AM, Rosner JL, Martin RG. Versatility of the carboxy-terminal domain of the alpha subunit of RNA polymerase in transcriptional activation: use of the DNA contact site as a protein contact site for MarA. Molecular microbiology. 2004; 54:45–59. [PubMed: 15458404]
19. Ross W, Gosink KK, Salomon J, Igarashi K, Zou C, Ishihama A, Severinov K, Gourse RL. A third recognition element in bacterial promoters: DNA binding by the alpha subunit of RNA polymerase. Science. 1993; 262:1407–1413. [PubMed: 8248780]
20. Schweimer K, Prasch S, Sujatha PS, Bubunenko M, Gottesman ME, Rosch P. NusA interaction with the alpha subunit of E. coli RNA polymerase is via the UP element site and releases autoinhibition. Structure. 2011; 19:945–954. [PubMed: 21742261]
21. Murakami KS. X-ray crystal structure of Escherichia coli RNA polymerase sigma70 holoenzyme. The Journal of biological chemistry. 2013; 288:9126–9134. [PubMed: 23389035]
22. Liu B, Zuo Y, Steitz TA. Structures of E. coli sigmaS-transcription initiation complexes provide new insights into polymerase mechanism. Proceedings of the National Academy of Sciences of the United States of America. 2016; 113:4051–4056. [PubMed: 27035955]
23. Opalka N, Chlenov M, Chacon P, Rice WJ, Wriggers W, Darst SA. Structure and function of the transcription elongation factor GreB bound to bacterial RNA polymerase. Cell. 2003; 114:335–345. [PubMed: 12914698]
24. Belogurov GA, Vassylyeva MN, Svetlov V, Klyuyev S, Grishin NV, Vassylyev DG, Artsimovitch I. Structural basis for converting a general transcription factor into an operon-specific virulence regulator. Molecular cell. 2007; 26:117–129. [PubMed: 17434131]
25. Martinez-Rucobo FW, Sainsbury S, Cheung AC, Cramer P. Architecture of the RNA polymerase-Spt4/5 complex and basis of universal transcription processivity. The EMBO journal. 2011; 30:1302–1310. [PubMed: 21386817]
26. Burmann BM, Knauer SH, Sevostyanova A, Schweimer K, Mooney RA, Landick R, Artsimovitch I, Rosch P. An alpha helix to beta barrel domain switch transforms the transcription factor RfaH into a translation factor. Cell. 2012; 150:291–303. [PubMed: 22817892]
27. Ma C, Mobli M, Yang X, Keller AN, King GF, Lewis PJ. RNA polymerase-induced remodelling of NusA produces a pause enhancement complex. Nucleic acids research. 2015; 43:2829–2840. [PubMed: 25690895]
28. Landick, R., Turnbough, CLJ., Yanofsky, C. Escherichia coli and Salmonella : Cellular and Molecular Biology. 2. Neidhardt, FC., editor. ASM; Washington DC: 1996. p. 1263-1286.
29. Kato T, Yoshida H, Miyata T, Maki Y, Wada A, Namba K. Structure of the 100S ribosome in the hibernation stage revealed by electron cryomicroscopy. Structure. 2010; 18:719–724. [PubMed: 20541509]
30. Ramrath DJ, Yamamoto H, Rother K, Wittek D, Pech M, Mielke T, Loerke J, Scheerer P, Ivanov P, Teraoka Y, Shpanchenko O, Nierhaus KH, Spahn CM. The complex of tmRNA-SmpB and EF-G on translocating ribosomes. Nature. 2012; 485:526–529. [PubMed: 22622583]

Author Manuscript Author Manuscript Author Manuscript Author Manuscript

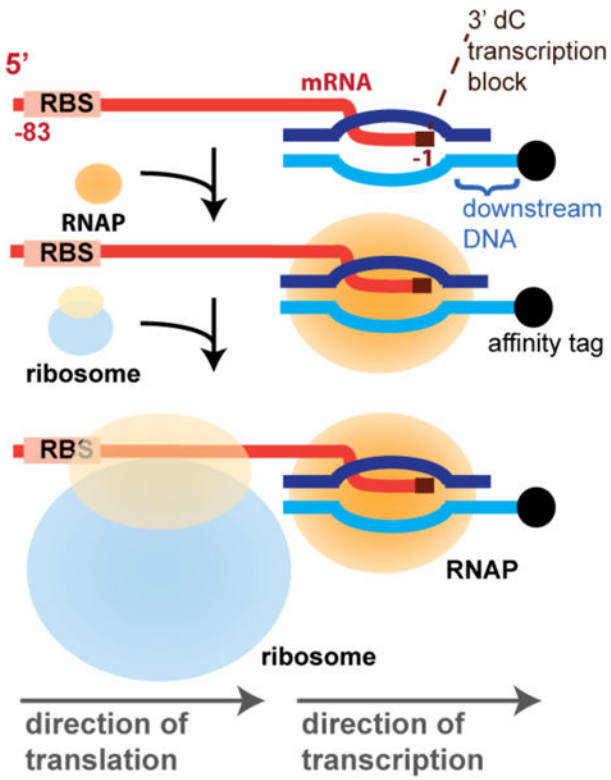

Fig. 1. Reconstitution of the expressome

Template DNA, non-template DNA and mRNA carrying a ribosome-binding sequence (RBS) and a 3′-desoxy-C (dC) end were annealed to obtain a nucleic acid scaffold. The mRNA register is indicated in red, where +1 is the nucleotide addition site in RNAP and negative numbers indicate upstream positions with respect to this site. RNAP was added to form a stalled transcription elongation complex (EC). The EC was then used as a template for *in vitro* translation. The ribosome translated the mRNA until encountering the stalled RNAP. Expressomes were purified from the reaction mix.

Author Manuscript Author Manuscript Author Manuscript Author Manuscript

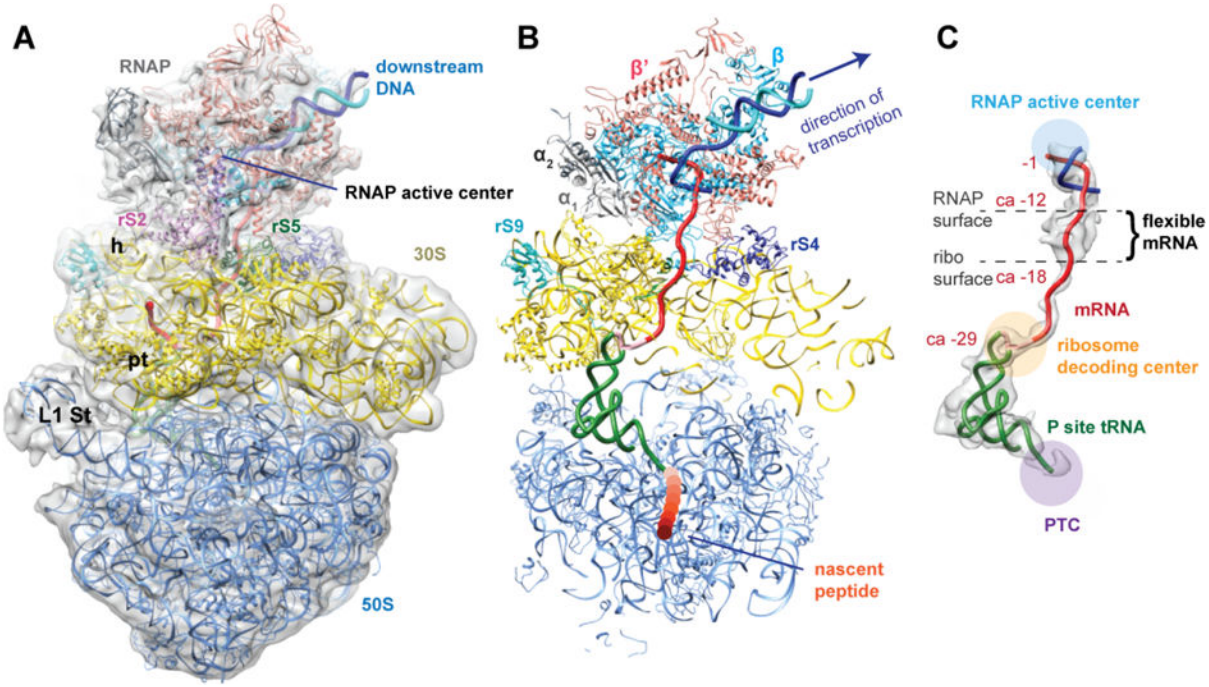

Fig. 2. Architecture of the expressome

(**A**) Cryo-EM reconstruction of the expressome. The electron density map was low-pass filtered to 9 Å resolution. Structures were rigid-body fitted. Ribosome landmarks are labeled in black (L1 St, L1 stalk; h, head; pt, platform). Color codes: 50S ribosomal subunit (blue), 30S (yellow). 30S proteins rS2 (pink), rS4 (dark blue), rS5 (forest green), rS9 (cyan), RNAP subunit α1 (light grey), α2 (dark grey), β (light blue), β′ (salmon), ω (light purple), template DNA (dark blue), non-template DNA (cyan), mRNA (red), codon and anticodon nucleotides (light rose), P-site tRNA (dark green), nascent peptide (orange). (**B**) Section through the fitted structures (PDB codes 2avy, 2aw4, and 5byh without αCTD) showing the path of mRNA (red) from the RNAP active center to the decoding center of the ribosome. The path of the nascent peptide chain is shown as orange dots (compare **Fig. S**). Same view as in (A). (**C**) Segmented density for template DNA, mRNA and tRNA. Nascent mRNA reaches the surface of the RNAP at ~register −12 and enters the ribosome at ~register −18. The mRNA codon nucleotides are at ~register −27 to −29.

Author Manuscript Author Manuscript Author Manuscript Author Manuscript

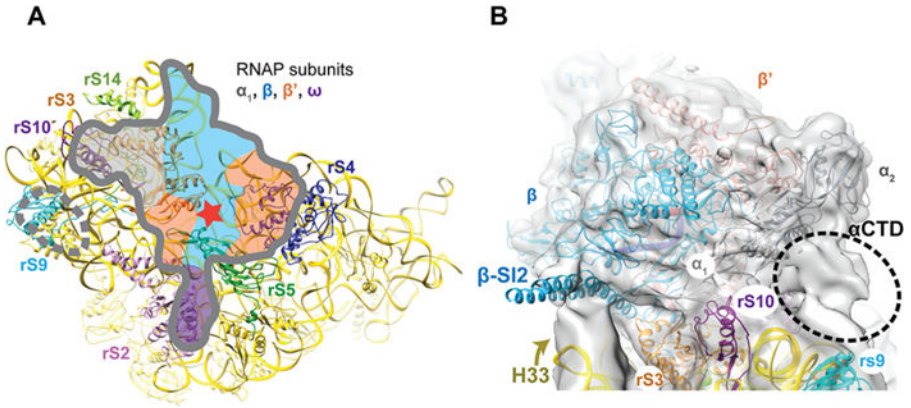

Fig. 3. RNAP-ribosome interactions

(**A**) Footprint of the RNAP on the solvent exposed surface of the 30S ribosomal subunit. View tilted 90° relative to Fig. 2A. Ribosomal proteins (rS2, rS3, rS4, rS5, rS9, rS10, rS14) are in different colors and labeled. The RNAP footprint on the 30S is outlined in grey and subdivided in regions contacting RNAP subunits. The dashed grey oval marks a putative αCTD contact site. The red star marks the entrance to the ribosomal RNA tunnel. (**B**) View of the RNAP-30S interface reveals an additional density attributed to the αCTDs (dashed oval). The αCTDs apparently contact 16S rRNA near h38 (~nt 1120) and h39 (~nt 1145) and rS9. The RNAP β-SI2 helix bundle (lower left) contacts H33 of the 16S rRNA. It is apparently mobile since the observed density does not fully cover the SI2 motif of the 5byh crystal structure. H33 moves towards RNAP relative to its location in the ribosome structure (PDB code 2avy, arrow). Relative to Fig. 2A, the view is rotated counterclockwise by 110° around the vertical axis.

Author Manuscript Author Manuscript Author Manuscript Author Manuscript

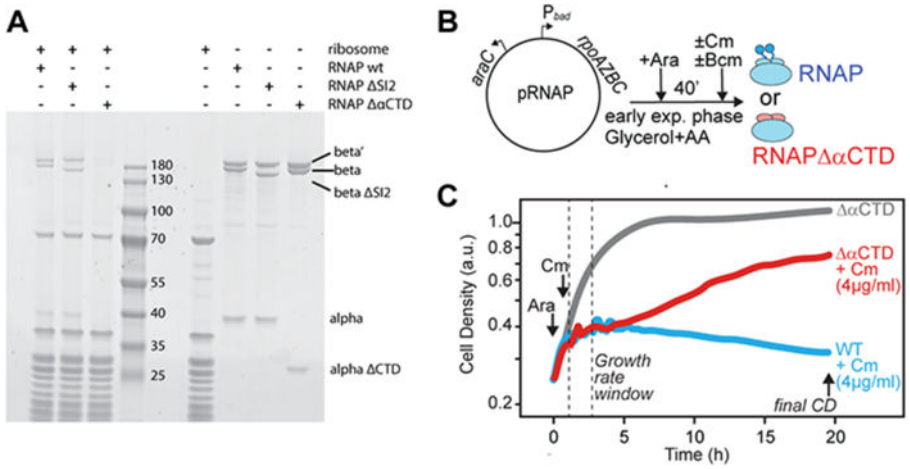

Fig. 4. RNAP-ribosome interaction is direct and functional

(A) RNAP variants were pre-incubated with 70S ribosomes at 1 μM concentration. Co-migration in a sucrose gradient was monitored by SDS-PAGE of ribosome-containing fractions (lanes 1–3). RNAP wt and RNAP ΔSI2 bind strongly to ribosomes, RNAP ΔαCTD shows strongly reduced binding, identifying the RNAP αCTD as an important binding module. To the right of the marker (lane 4), loading controls show the expected molecular weight of the proteins (lanes 5–8). **(B)** RNAP (wild-type or lacking the αCTD) was expressed from plasmids under control of the P_{bad} promoter in minimal medium. After 40 minutes of expression, chloramphenicol (Cm), bicyclomycin (Bcm), or both was added to inhibit ribosomes and ρ termination factor, respectively. **(C)** Cell density with time for cultures with or without Cm at 4 μg/ml. The reduction in the effect of Cm became more pronounced upon longer incubation.